

Simulation of Time Series Received Underwater from Small Explosive Detonations in Shallow Ocean Regions

Adrian D. Jones (1) , Alec J. Duncan (2) , Paul A. Clarke (3) and Amos Maggi (2)

(1) Program Office, DSTO Edinburgh, SA 5111, Australia

(2) Centre for Marine Science & Technology, Curtin University of Technology, Perth WA 6845, Australia

(3) Maritime Operations Division, DSTO Edinburgh, SA 5111, Australia

ABSTRACT

The sound pressure time series received at medium ranges from small underwater explosives, known as "SUS" charges, have been under close study in recent years in relation to the potential impact of the use of such devices on marine fauna, in particular, marine mammals. Past work has centred on investigations of time series measured in shallow oceans in the Australian region. Here, at-sea measured data showed, consistently, received peak levels which were considerably less than published weak shock theory would have suggested. This paper shows the results from the analysis of an extended data set, which includes measurements of SUS signals received along a shallow ocean track in an additional ocean region. Further, this paper shows the results of simulations of the time series received along all these tracks. These simulations of received SUS waveforms, carried out at Curtin University, have been obtained by generating an inverse Fourier transform of the product of the oceanic transfer function and the Fourier transform of an input SUS waveform. The oceanic transfer function has been based on the use of the SCOOTER model at low frequencies and a ray model (BELLHOP gaussian beam ray model) at remaining frequencies. By simulating the received time series in this way, reasons for the discrepancies between measured peak data and expectations based on weak shock theory have been investigated and are presented in this paper.

INTRODUCTION

Underwater explosive devices have a long history of use as sonar signal sources by defence forces internationally (see, for example, Urick 1983 figure 1.3 and section 4.4). A number of standardised designs were developed for Signal Underwater Sound (SUS) explosive sources, these differing in the weight of the explosive charge and in the depth in the ocean at which detonation was pre-set to occur.

The use of SUS as signal sources for anti-submarine warfare (ASW) has, for several decades, been replaced by the use of coherent sources, capable of generating tonal signals of extended duration. However, the SUS charge remains an attractive option as a signal source for characterising the acoustic parameters of a shallow ocean region (eg. transmission loss and reverberation (eg. Hall 1996)). Underwater explosives, such as SUS, are an anthropogenic noise source type which has potential to cause harm or annoyance to marine fauna. As the Australian Defence Force (ADF) wishes to conduct its maritime operations in an environmentally responsible manner, DSTO in conjunction with Curtin University, has been conducting research to understand relevant phenomena and establish essential principles. This paper shows recent results of this work, and provides an update to descriptions published previously by Jones and Clarke (2004, 2005).

BACKGROUND TO PRESENT WORK

Previous work (Jones and Clarke 2004, 2005) presented measurements of signals received from SUS for two shallow ocean tracks – Track A and Track B. It was shown that the broadband acoustic signal energy received at ranges from several km to about 10 km was in accord with expectations, whereas the broadband peak level received was much less than anticipated for a quiescent ocean of infinite extent. Here, the differences between theory and measurement exceeded 10 dB and approached 20 dB. The reason for this

discrepancy was not known with certainty, but it was not considered to be due to a lack of data integrity. It was postulated that the reduced peak level might be due to one or more of the following: lack of coherence in transmission due to medium irregularities; lack of coherence of reflection due to boundary irregularities. A lack of coherence would be associated with time spreading, enhancing the possibility of pulse reduction.

To further investigate the relevant phenomena, it was decided to (1) analyse pressure time series data for an additional ocean track, (2) simulate received time series for all measurement scenarios and (3) simulate effects of a small degree of loss of coherence in transmission.

MEASURED DATA FOR TRACK C

Underwater signals received from SUS charges have been obtained along a number of tracks within continental shelf waters in the Australian region. For each track, *in-situ* details include water temperature versus depth for at least one point along the track (from which sound speed versus depth has been obtained). All signals selected for analysis were examined for the presence of overload and any exceeding system criteria were rejected (Valentine Flint and Lawrence 1992). In addition, data were selected for study only if the peak level throughout the entire measured waveform was at least 5.5 dB less than the hard clipping limits of the recording system. This latter criterion was selected, as these requirements exceed the maximum possible amount by which the data sampling rate of 20 kHz might cause a peak from the SUS type in question to be underestimated. Here, the peak waveform has been assumed to be in the shape of an instantaneous rise followed by an exponential decay, with a time constant of 0.1 ms, this being applicable to ranges greater than several km. Using this criterion, data reported at 2.2 km on Track A (Jones and Clarke 2004) are now rejected.

Data for Track C were obtained using a receiver at 18.3 m depth with SUS detonated at 18.3 m depth for ranges to 10 km. The data sampling rate was 20 kHz, giving a maximum frequency, taking account of anti-alias filtering, of 8kHz. Ocean depth was near constant along the track at 55 m. The sound speed profiles at the start and end of the 21.9 km track are shown in Figure 1. An acoustic ray diagram to 6 km along the Track is shown in Figure 2. This is based on the “start” sound speed profile, as the 6 km represents a small proportion along the track. Received pressure time series at the closest range point for valid data (5.59 km) are shown in Figures 3 and 4. Data at 10.7 km range are shown in Figures 5 and 6.

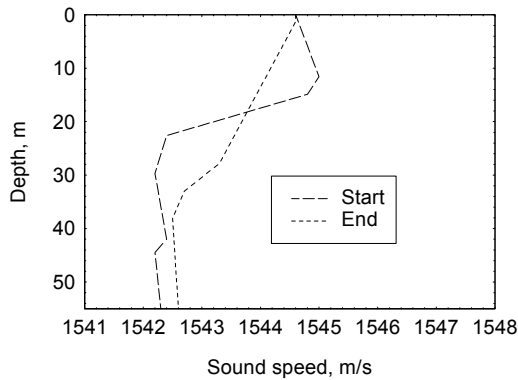


Figure 1. Sound speed profile for Track C

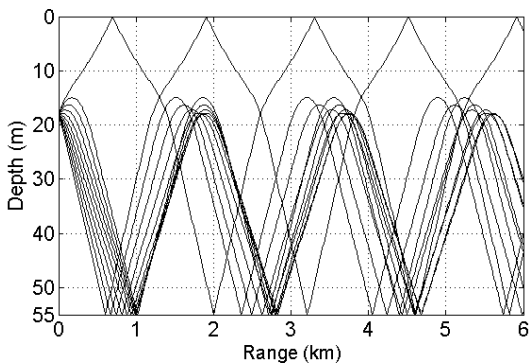


Figure 2. Acoustic ray diagram for sound radiated from source for Track C, 11 rays over ± 2½ degrees

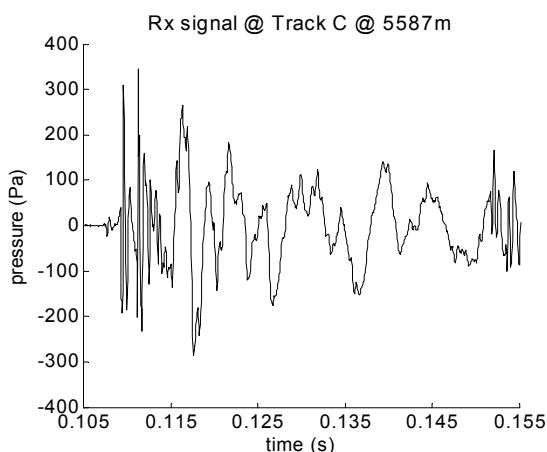


Figure 3. Received sound pressure time series, Track C, initial 0.05 s, 5.59 km

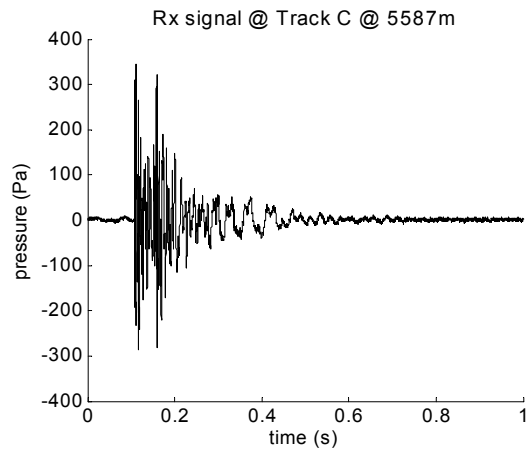


Figure 4. Received sound pressure time series, Track C, full pulse, 5.59 km

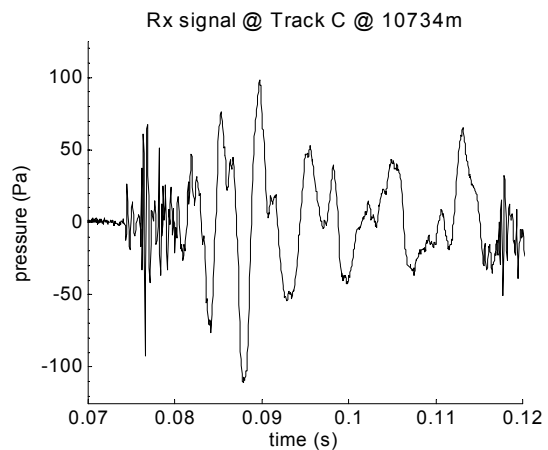


Figure 5. Received sound pressure time series, Track C, initial 0.05 s, 10.7 km

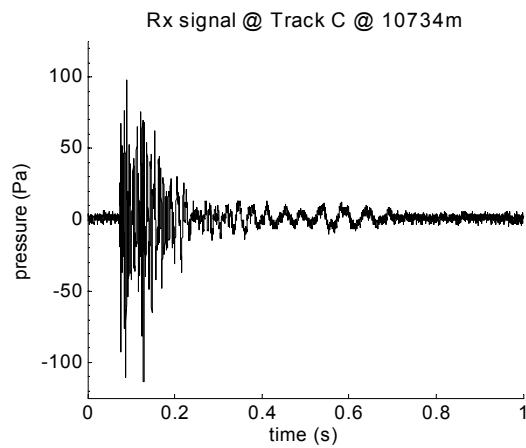


Figure 6. Received sound pressure time series, Track C, full pulse, 10.7 km

Table 1. Measured and predicted received SUS sound pressure data for shallow water Track C

	Horizontal range	
	5.59 km	10.7 km
Peak pressure P_0 (measured)	345 Pa	114 Pa
Peak pressure P_0 (theoretical)	1350 Pa	690 Pa
Measured broadband peak level, dB re $(1 \mu\text{Pa})^2$	171 dB	161 dB
Theoretical broadband peak level, dB re $(1 \mu\text{Pa})^2$	183 dB	177 dB

Received Peak Pressure

Measured and theoretically predicted peak pressure data are shown in Table 1. The theoretical predictions were obtained from weak shock theory (Rogers 1977), as described by Jones and Clarke (2004), and neglect the effects of refraction.

Data in the first two rows show that the amplitude of the received pressure peak, measured at each range value, is considerably less than that predicted from weak shock theory for a direct path arrival at the corresponding range. This discrepancy is a factor of 4 (12 dB) in the data at 5.59 km range, and a factor of 6 (16 dB) in the data at 10.7 km range. These differences are also typical of those observed by Jones and Clarke (2004, 2005) for Tracks A and B.

The ray plot in Figure 2 shows that the first arrivals must have travelled via a number of surface and bottom bounces. It may then be expected that the peak pressure is reduced by surface and bottom losses, relative to the expectation for a direct arrival, but it may also be expected that surface roughnesses and random inhomogeneities in the water column (eg. section 6.2 of Tolstoy and Clay 1987) will each be possible causes of losses of coherence and contribute to the total peak reduction.

Data Acquisition

The measurement system for Track C had a flat frequency response from about 7 Hz to 8 kHz. The receiver amplifier output permitted the recording of undistorted peak acoustic pressures of 179.9 dB re $(1\mu\text{Pa})^2$ (± 989 Pa). Soft clipping of acoustic signals occurred above this limit, with hard clipping occurring at 181.1 dB re $(1\mu\text{Pa})^2$ ($\pm 1,135$ Pa). Using the criterion mentioned above, measured and replayed SUS data must be at least 5.5 dB less than the hard clipping limit for the data to be considered free from any possible clipping distortion. For Track C, this effective limit for data is 175.6 dB re $(1\mu\text{Pa})^2$ (± 603 Pa). The data shown above clearly fit well beneath this limit, and in fact at 10.7 km the maximum value theoretically possible for a direct arrival very nearly fits within this limit.

TIME SERIES SIMULATION

Reasons for Simulations

The peak pressure data for Track C follow the trend already observed for Tracks A and B (Jones and Clarke 2004, 2005) in that the measured peak values are considerably less than those predicted by weak shock theory for direct path arrivals in an ocean of uniform water column properties. In order to investigate the cause(s) of these differences, it was decided to perform simulations of the transmitted time series for all three ocean tracks and to study potential causes in turn.

SUS Source Time Series Model

A model source time series was required at the standard 1 m distance so that the transmitted waveform might be found using linear acoustic transmission models. This was complicated by the fact that the sound pressure waveforms radiated by explosions are known to be subject to non-linear shock phenomena (eg. Urick 1983). For the present work, a waveform peak amplitude was determined using theory applicable to explosive sources at a distance r_x beyond which linear acoustic transmission was assumed. The source time series was then determined by assigning an equivalent peak pressure at a range 1 m by assuming a time reversal back-

propagation with $1/r$ type spreading from range r_x . The value of r_x was taken as 1000 m.

The expression used to determine the peak amplitude P_0 was that of Urick (1983), which is also equation (9) of Jones and Clarke (2004). This yielded a source peak pressure of 5.77 MPa or 255 dB re $(1\mu\text{Pa})^2$ s at 1m. Note that this Source Level results in peak pressure values P_0 which are 2.3 dB and 2.1 dB less, respectively, than the effective Source Level peak values implied by back-propagation from the theoretical values shown in Table 1. These theoretical values were determined using the weak shock theory of Rogers (Jones and Clarke 2004). The source waveform used for the present work is shown in Figure 7. The assumed form of bubble pulses (eg. Urick 1983) is shown in the upper part of Figure 7, the initial pulse is shown in the lower part. The SUS source was modelled as detonated at depth 18.3 m.

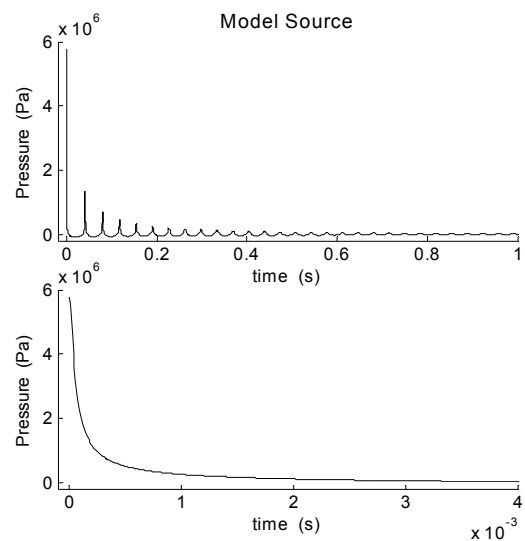


Figure 7. Model source signal used in this work

Simulations of Received Signals

Received SUS waveforms were simulated by generating an inverse Fourier transform of the product of the oceanic transfer function and the Fourier transform of the input SUS waveform (Figure 7). The oceanic transfer function was based on the models SCOOTER (fast-field model) at low frequencies and BELLHOP (gaussian beam ray model) at remaining frequencies. These calculations required separate transfer functions to be determined for each field point at which SUS data exists for each ocean track. SCOOTER and BELLHOP were used so that an elastic substrate might be modelled for what were assumed to be constant depth ocean scenarios.

The wave model and ray model transfer functions were constructed separately and compared to determine a suitable crossover frequency. SCOOTER was run at 1 Hz increments from 1 Hz to 800 Hz. BELLHOP was run using 1021 rays launched over a range of $\pm 85^\circ$ from the horizontal (angular spacing of $1/6^{\text{th}}$ of a degree) and at a frequency of 1 kHz. The output amplitude-delay information was used to generate transfer function ordinates across the entire 20 kHz bandwidth at 1 Hz increments. A crossover band of 100 Hz centred on 750 Hz was selected to merge the transfer functions, with a linear weight function used to calculate the complex mean at each frequency. The crossover bandwidth was selected to minimise the Gibbs phenomenon-related ringing in the overall impulse response induced by mismatch between low and high frequency transfer functions.

All data considered in this paper were received at a depth of 18.3 m. All simulated data were determined to an upper frequency limit of 20 kHz and then low pass filtered to 8 kHz to simulate the anti-alias filter frequency of 8 kHz used for the measurements.

SIMULATIONS AND DATA FOR TRACK A

The Track A environment (Jones and Clarke 2004) was modelled using a uniform depth of 56.5m. Based on a sediment surface sample of fine silt, an upper substrate of fine silt was modelled using parameters listed in Table 1.3 of Jensen et al. (1994) including a depth-dependent shear velocity $c_S(z)$ ms^{-1} according to $c_S(z) = 80z^{0.3}$, to a layer depth z of 259 m. The remainder of the substrate was treated as a limestone halfspace, using parameters listed in Table 1.3 of Jensen et al. (1994). The resultant reflection coefficient and phase angle data are shown in Figure 8. The sound speed profile measured at the start of the track (Jones and Clarke 2004) was used for modelling the water column.

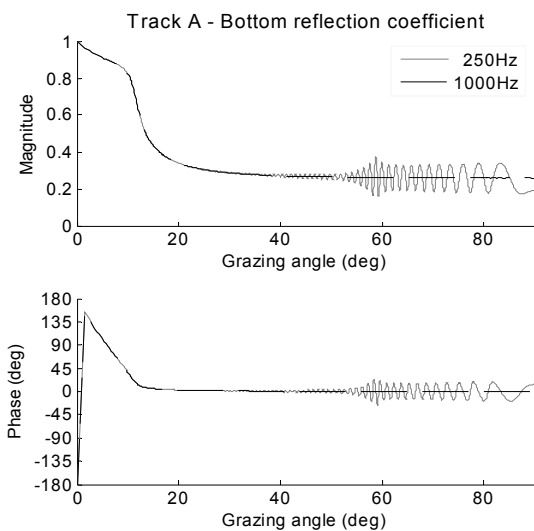


Figure 8. Seafloor reflection coefficient for Track A

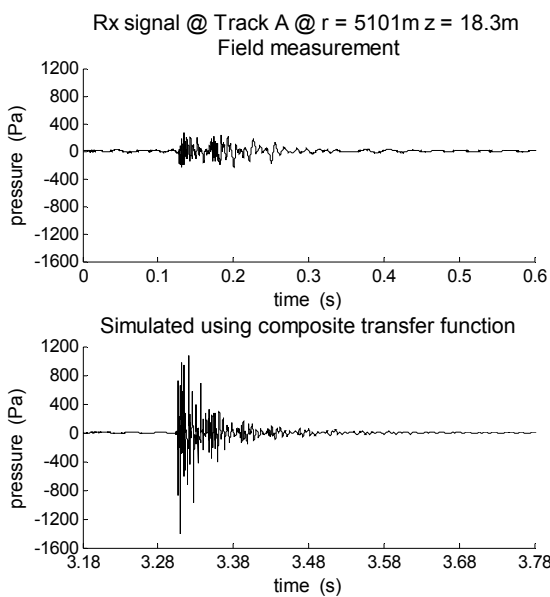


Figure 9. Measured & simulated waveforms, 5.10 km, Track A

The reflection data implied by Figure 8 for shallow angles are very close to those obtained for the same track by an acoustic

inversion analysis (Jones et al 2002). This track was previously labelled as “AE”.

The measured and simulated time series waveforms for the first valid range point along Track A, at 5.10 km, are shown in Figure 9. The leading edge detail of these time series data is shown in Figure 10. The measured and simulated time series waveforms for the next range point along Track A, at 10.1 km, are shown in Figure 11. The leading edge detail of these time series data is shown in Figure 12.

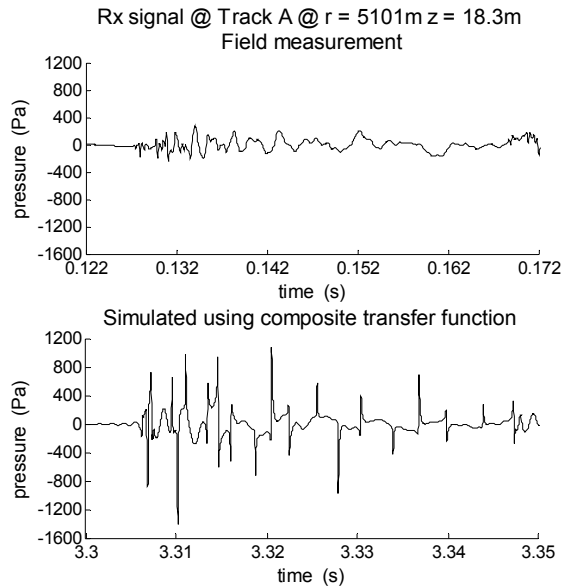


Figure 10. Measured & simulated waveforms, 5.10 km, Track A – detail of initial pulse
b

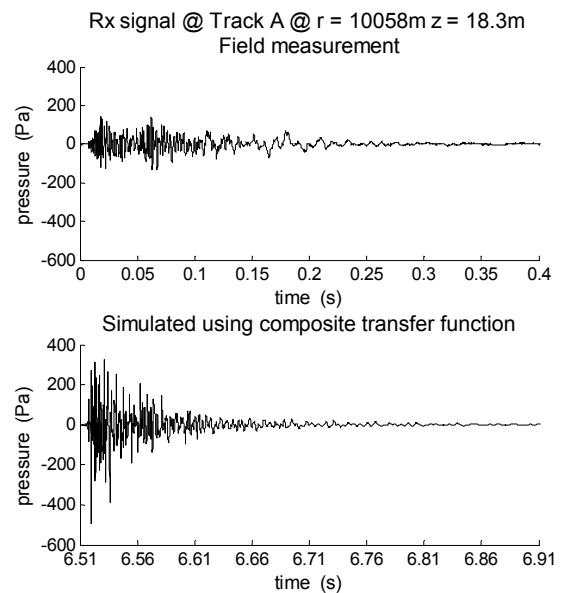


Figure 11. Measured & simulated waveforms, 10.1 km, Track A

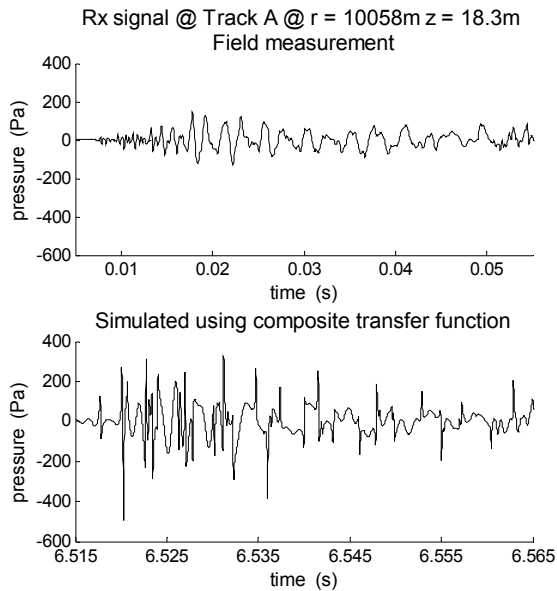


Figure 12. Measured & simulated waveforms, 10.1 km, Track A – detail of initial pulse

Discussion

Close inspection shows that, apart from the magnitude of the sharp peaks, the simulations are accurate in estimating the duration, amplitude and character of the features of the waveforms at both range values. The amplitudes of the peak excursion data, as simulated, are much greater than observed in the measurements, and the largest peak excursions are just a few dB less than predictions based on weak shock theory for direct arrivals (Jones and Clarke 2004).

In earlier work (Jones and Clarke 2004, 2005) it was suggested that peak values associated with such short duration impulses might be spread in time, slightly, due to non-specular reflections from boundaries and due to thermal microstructure effects. Any such time spreading would result in some reduction of peak values and the simulations would be expected to be much closer to the measured data. This was investigated and the work is reported later in the paper.

SIMULATIONS AND DATA FOR TRACK B

The Track B environment (Jones and Clarke 2005) was modelled using a uniform depth of 94 m. An upper substrate of silt was modelled using parameters listed in Table 1.3 of Jensen et al. (1994) including a depth-dependent shear velocity $c_S(z)$ ms^{-1} according to $c_S(z) = 80z^{0.3}$, to a layer depth z of 500 m. The next layer was a halfspace with constant shear velocity at the 500 m depth level (750ms^{-1}). The resultant reflection coefficient and phase angle data is shown in Figure 13. The sound speed profile measured at the start of the track (Jones and Clarke 2005) was used for modelling the water column.

For shallow angles, this reflection data is representative of a bottom loss vs. grazing angle slope of about 35 dB/radian at all frequencies. The acoustic inversion technique reported by Jones et al (2002), when applied to this track, gave similar slope at 4 kHz (32.8 dB/radian), but lower slope at lower frequencies (18.4 dB/radian at 2 kHz, 13 dB/radian at 1 kHz and 500 Hz), corresponding to a more reflective seabed at lower frequencies. The measured and simulated time series waveforms for the first valid range point along Track B, at 3.51 km, are shown in Figure 14. The leading edge detail of these time series data are shown in Figure 15.

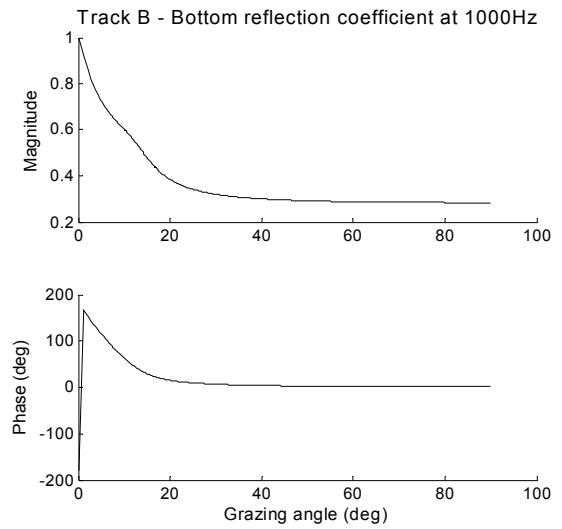


Figure 13. Seafloor reflection coefficient for Track B

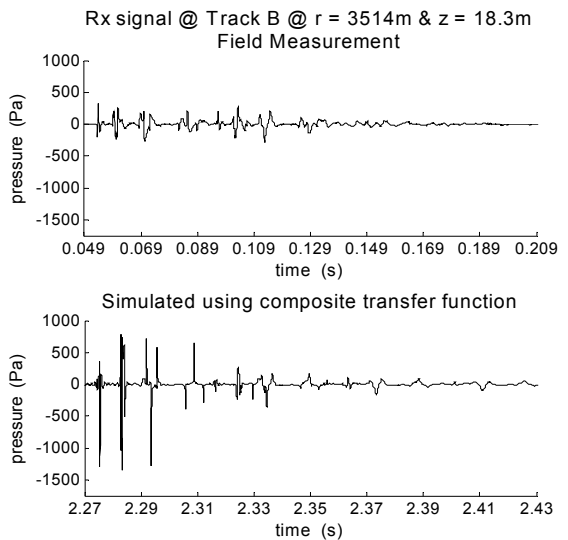


Figure 14. Measured & simulated waveforms, 3.51 km, Track B

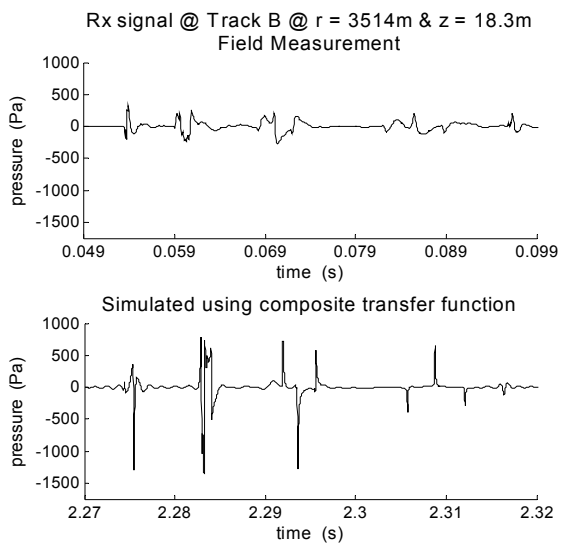


Figure 15. Measured & simulated waveforms, 3.51 km, Track B – detail of initial pulse

Discussion

As for Track A, inspection of the waveforms for Track B shows the simulation to be reasonably accurate in the

duration, amplitude and character of the general features of the time series. The exception is the amplitude of the sharp peaks in the simulation which greatly exceed the measured data. For Track B, the largest peak excursion is just 4 dB less than a prediction based on weak shock theory for direct arrivals (Jones and Clarke 2005).

SIMULATIONS AND DATA FOR TRACK C

Track C was modelled using a uniform depth of 55 m. An upper substrate of silt was modelled as for Track B. As for Track B, the next layer was a halfspace with constant shear velocity at the 500 m depth level (750ms^{-1}). The resultant reflection coefficient and phase angle data are shown in Figure 16. The sound speed profile measured at the start of the track was used for modelling the water column.

The reflection data implied by Figure 16 for shallow angles is representative of a bottom loss slope of about 40 dB/radian at all frequencies. The acoustic inversion technique reported by Jones et al (2002), when applied to this track, gave similar slope at 4 kHz (55 dB/radian), but lower slopes at lower frequencies (32 dB/radian at 2 kHz, 21 dB/radian at 1 kHz and 8.9 dB/radian at 500 Hz).

The measured and simulated time series waveforms for the first valid range point, at 5.59 km, are shown in Figure 17. The leading edge detail is shown in Figure 18.

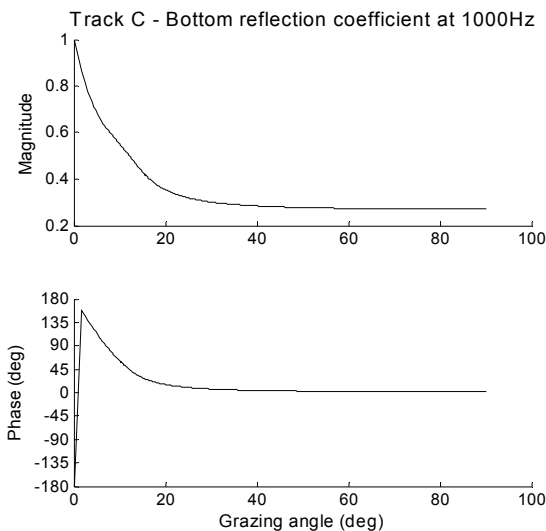


Figure 16. Seafloor reflection coefficient for Track C

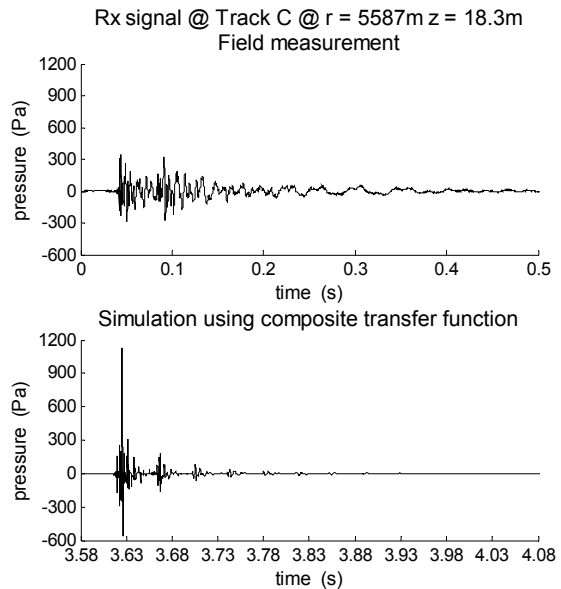


Figure 17. Measured & simulated waveform, 5.59 km, Track C

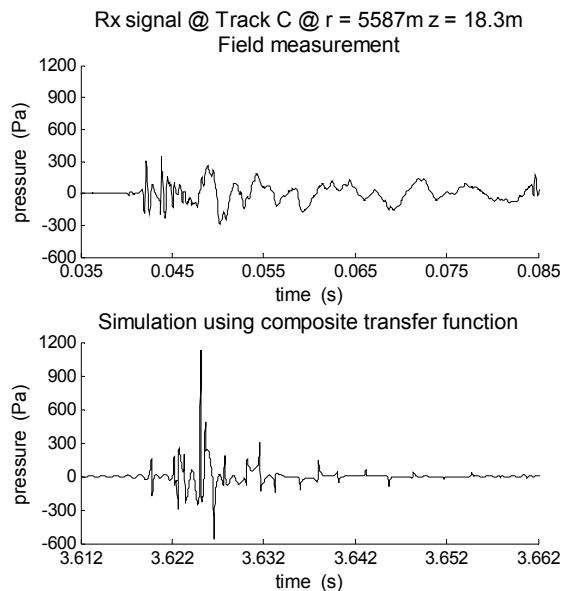


Figure 18. Measured & simulated waveform, 5.59 km, Track C – detail of initial pulse

Discussion

The simulations for Track C are, generally, less representative of the measured data than those for the other tracks. To some degree, it is believed that this is due, in part, to an overestimation of seafloor reflection losses. The simulations show bursts of energy separated by about 40 ms, and of successively decreasing amplitude. As the bubble pulse period for this SUS type at 18.3 m depth is known to be about 40 ms, it may be assumed that these bursts correspond to the initial peak and the bubble pulse peaks (ref. bubble pulses in modelled source waveform, Figure 7). It thus appears that modelling of Track C has under-estimated the reflectivity of the actual seafloor, as the measured data show the bursts of energy associated with the initial pulse and bubble pulses as coalescing – indicating that the higher order transmission multi-paths are only weakly attenuated at subsequent seafloor reflections. Similarly as for the other tracks, the largest peak excursions are just a few dB less than predictions based on weak shock theory for direct arrivals.

PEAK PRESSURE DATA

Peak pressure data obtained from the simulations above, and from measurements shown above for Track C, and as published earlier for Track A (Jones and Clarke 2005) and Track B (Jones and Clarke 2005) are shown in Table 2. Here, the peak value shown for each range point for each track is the highest excursion, either +ve or -ve. The theoretical values are those attributed to a direct arrival in a quiescent uniform ocean of infinite extent, based on weak shock theory as described by Rogers (1977).

Table 2. Measured and predicted received SUS sound pressure data for shallow water Tracks A, B and C

Ocean Track	Range (km)	Measured peak (Pa)	Simulated peak (Pa)	Theoretical Peak (Pa)
Track A	5.10	268	1413	1490
	10.1	146	498	732
Track B	3.51	319	1351	2200
Track C	5.59	345	1132	1350
	10.7	114	393	690

The data shown in the 3rd and 5th columns indicates that the measured peak values are much less than weak shock theory suggests for a direct arrival. However, the simulations, which are carried out assuming perfect specular reflection from boundaries and exclude effects of water column inhomogeneities, clearly show an expectation of peak values close to those from weak shock theory.

In order to investigate whether the reduced peak values in the 3rd column relative to the data in the 4th and 5th columns are influenced by (i) choice of seafloor reflectivity, (ii) transmission micro-paths, other simulations were performed.

EFFECT OF ALTERNATE SEAFLOOR

The effect of an alternate modelling of the seafloor was investigated for Track B. A much more reflective seafloor was modelled with a medium sand substrate using parameters listed in Table 1.3 of Jensen et al. (1994) including a depth-dependent shear velocity $c_S(z)$ ms⁻¹ according to $c_S(z) = 110z^{0.3}$, to a layer depth z of 500 m. This was modelled as over a halfspace with constant shear velocity at the 500m depth level (750ms⁻¹). The resultant reflection coefficient and phase angle data are shown in Figure 19.

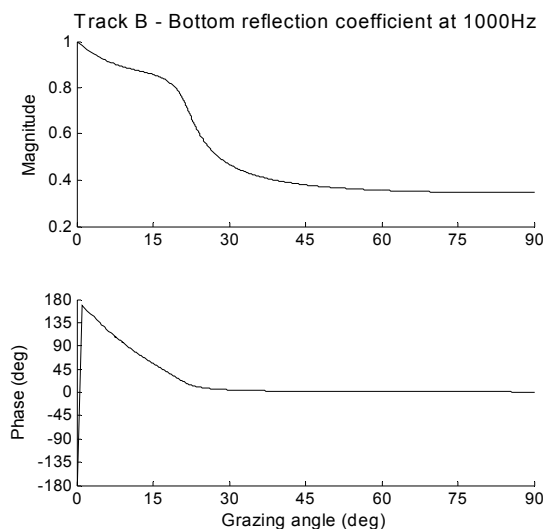


Figure 19. Seafloor reflection coefficient for alternate seafloor for Track B

These reflection data, at shallow angles, are representative of a bottom loss slope of about 6 dB/radian at all frequencies, indicating a much greater reflectivity than determined by the acoustic inversion analysis reported by Jones et al (2002) which gave 32.8 dB/radian at 4 kHz, 18.4 dB/radian at 2 kHz, 13 dB/radian at both 1 kHz and 500 Hz.

Waveforms at 3.51 km range are shown in Figure 20. This figure is directly comparable with Figure 14. Both show time series data for 0.16 seconds of the received SUS signal. The data for the more reflective seafloor has simulated peak values which are greater than those for the original seafloor, plus the overall level of the general waveform amplitude is much greater for the reflective seafloor and is no longer a reasonable representation of the measured waveform. Clearly, this changed seafloor reflectivity has a significant effect on both the total energy and peak values.

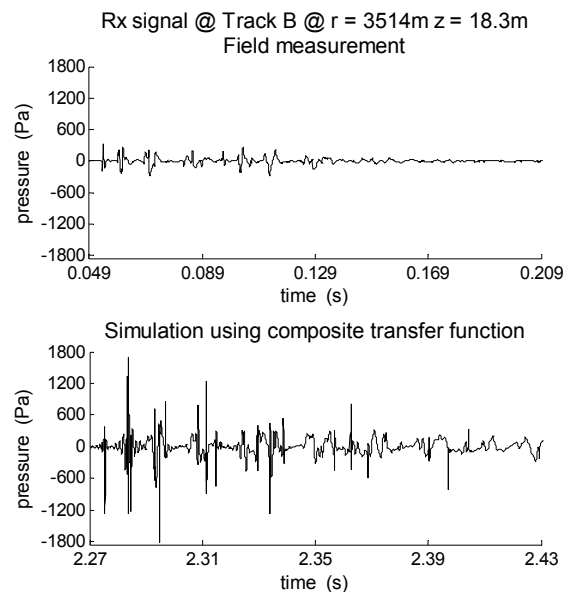


Figure 20 Measured & simulated waveform, 3.51 km, Track B, reflective seafloor

TEMPORAL COHERENCE EFFECTS

The real transmission environment may be expected to include slight, random, time spreading due to phenomena such as non-specular reflection from the sea surface and seafloor, and due to thermal microstructure and other non-homogeneities within the ocean. This may be considered as transmission along a number of micro-paths connecting the transmitter and receiver, each with a slightly different transmission delay. Signals travelling along the different micropaths then sum at the receiver. Above a sufficiently high frequency, the spread in micro-path delays becomes larger than the period of the signal and the components add with random phase, which may be considered as a loss of coherence. A consequence of the time spread will be a reduction in the amplitude of sharp peaks. To investigate the likelihood of this phenomenon, simulations of micro-path transmission were made for Track A.

The simulation is carried out as follows: For each field point, the rays determined by the ray model (BELLHOP) are each divided into M micropaths all of amplitude $1/M$ and each is assigned, at random, an additional time delay or advance drawn from a Gaussian distribution with zero mean and standard deviation σ_i seconds. An equivalent transfer function $H(f)$ is then computed from

$$H(f) = \sum_{p=1}^N \sum_{q=1}^M a_{p,q} \exp(2\pi i f \tau_{p,q}), \quad \text{where } f \text{ is}$$

frequency, $a_{p,q}$ and $\tau_{p,q}$ are the amplitude and propagation delay for micropath q of ray path p , N is the number of ray-paths and M is the number of micropaths. This transfer function is then combined with that obtained from the wave model (SCOOTER) as described above.

This technique assumes that the micro-path structure is constant across the pulse duration and that all ray multi-paths have the same time-spread. This second assumption is unlikely to be correct, as different ray paths have different numbers of boundary interactions, but is a reasonable starting point. Each waveform realisation is non-unique, as a different set of random samples may be taken, however, if the number of micro-paths per ray M is very large, all realisations are effectively the same. A time series thus simulated for the first range point for Track A, based on 100 micro-paths, is shown in Figure 21 together with the original simulation without the micro-paths.

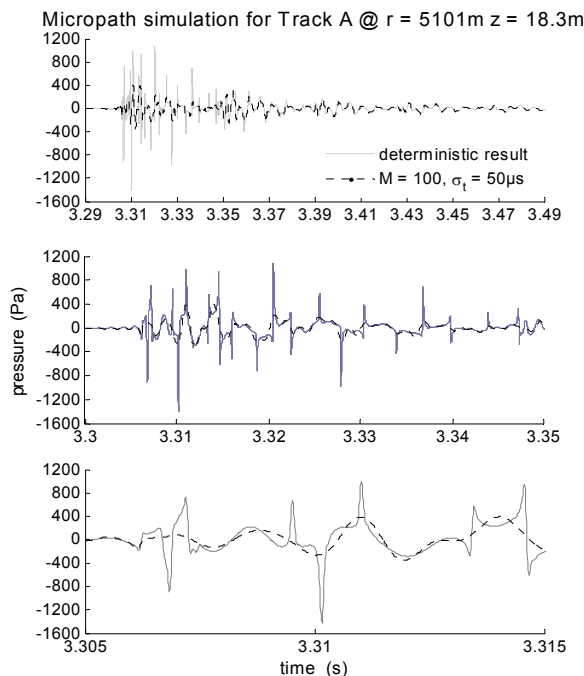


Figure 21 Waveforms simulated without (solid line) and with (broken line) micro-paths, 5.10 km, Track A

The micro-path data were obtained with the time delay standard deviation σ_t set to 0.05 ms for all ray multi-paths. For this test case, peak reduction became independent of M at around $M \in [50, 100]$. Clearly, this degree of micro-path phenomena has reduced the amplitude of peak pressure excursions, whilst having little effect on the lower frequency components of the waveform. The maximum peak excursion for the micropath data is 394 Pa, whereas the non-micropath simulation gave 1413 Pa (Table 2).

DISCUSSION

The results of the simulations for all three Tracks A, B and C do show that the SUS peak pressure excursion levels predicted on the assumption of specular reflection from the sea surface and seafloor, and the assumption of no ocean inhomogeneities, are close to levels obtained from weak shock theory. These simulations do not reproduce the small peak levels of the measured data. However, the data for Tracks A and B do tend to indicate that the SUS waveform

components other than sharp peaks may be simulated with good levels of accuracy, in amplitude and timing, using phase coherent transmission models with an accurate representation of the seafloor reflectivity.

The simulation of micro-paths does suggest that, if such transmission events are modelled, the peak levels obtained by modelling may be closer to measured data. To some degree, this reduction in amplitude of the simulated peak levels is obvious, in that the micro-path phenomena amounts to a convolution of the transmitted pulse with the time spread of the micro-pathing. This convolution may be shown to apply a low-pass filter to the data, hence the obvious reduction of sharp peaks. Simulations not shown here do suggest that the degree of low-pass filtering is influenced by the number of micro-paths.

Present investigations are centred on theoretical examination of the degree to which thermal microstructure within the water column, and roughness of boundary surfaces will cause time spreads to transmitted pulses.

CONCLUSIONS

This study presents data for an additional shallow ocean track which corroborates previous reports (Jones and Clarke 2004, 2005) that measured peak pressures received from SUS in shallow water at medium range are much lower than predicted by weak shock theory. This study also shows that the general features of waveforms received from SUS in shallow water may be predicted with good levels of accuracy using phase coherent transmission models with assumptions of a quiescent ocean and smooth boundaries, however, modelled peak values are much greater than available measured data and are close to weak shock predictions. Predictions of peak values can be brought much closer to observed peak data if temporal spreading effects are included, but an investigation of the plausibility of the required amount of spreading is ongoing.

REFERENCES

- Hall, M.V. 1996 *Measurement of Seabed Sound Speeds from Head Waves in Shallow Water*, IEEE Journal of Oceanic Engineering, Vol. 21, No. 4, pp 413 – 422
- Jensen, F.B., Kuperman, W.A., Porter, M.B., Schmidt H., 1994 *Computational Ocean Acoustics* AIP Press
- Jones, A.D. and Clarke P.A. 2004 *Underwater Sound Received from some Defence Activities in Shallow Ocean Regions*, Proceedings of ACOUSTICS 2004, Gold Coast, Australia, pp 467 – 473
- Jones, A.D. and Clarke, P.A. 2005 *Peak Levels from SUS Measured in Shallow Oceans in the Australian Region*, Intl. Conf. on Underwater Acoustic Measurements: Technologies and Results, Heraklion, Crete
- Rogers, P.H. 1977 *Weak-shock solution for underwater explosive shock waves* J. Acoust. Soc. America, Vol. 62, No. 6, pp 1412 – 1419
- Tolstoy, Ivan and Clay, C.S. 1987 *Ocean Acoustics Theory and Experiment in Underwater Sound*, American Institute of Physics
- Urick, R.J. 1983 *Principles of Underwater Sound*, 3rd edition, McGraw-Hill
- Valentine Flint, S. and Lawrence, M.W. 1992 *Bottom bounce propagation on SEAMAP Pacific routes: Data acquisition and recording system* DSTO MRL-TN-587